NASA TECHNICAL NOTE

NASA TN D-2190

NASA TN D-2190
C. 1

SUPERSONIC LONGITUDINAL STABILITY CHARACTERISTICS OF THE TWO FINAL STAGES OF A FOUR-STAGE LAUNCH VEHICLE

by Royce L. McKinney

Langley Research Center
Langley Station, Hampton, Va.

NATIONAL AERONAUTICS AND SPACE ADMINISTRATION • WASHINGTON, D. C. • MARCH 1964

SUPERSONIC LONGITUDINAL STABILITY CHARACTERISTICS OF THE TWO FINAL STAGES OF A FOUR-STAGE LAUNCH VEHICLE

By Royce L. McKinney

Langley Research Center
Langley Station, Hampton, Va.

NATIONAL AERONAUTICS AND SPACE ADMINISTRATION

For sale by the Office of Technical Services, Department of Commerce,
Washington, D.C. 20230 -- Price $0.50

SUPERSONIC LONGITUDINAL STABILITY CHARACTERISTICS OF THE TWO FINAL STAGES OF A FOUR-STAGE LAUNCH VEHICLE

By Royce L. McKinney

SUMMARY

Tests were conducted in the Langley Unitary Plan wind tunnel on the third and fourth stages of the spacecraft-orientation-control-system (SOCS) launch vehicle with a cone-cylinder nose. Two fin sizes and two shapes of a small fairing ring on the nose were tested at Mach numbers of 2.30, 2.96, 3.96, and 4.65 throughout an angle-of-attack range from approximately -7° to 7° at an angle of sideslip of 0°. The Reynolds number for the test was 2×10^6 per foot.

The results of the investigation indicated regions of instability for the configuration with small fins. However, the configuration with large fins and both with and without the fairing rings provided a satisfactory margin of stability throughout the Mach number range of the investigation.

INTRODUCTION

The model tested represents the third and fourth stages of the spacecraft-orientation-control-system (SOCS) launch vehicle. The nose consisted of a cone with a hemispherical nose and a short cylinder with length and diameter equal to the diameter of the fourth-stage propulsion unit. At the aft end of the nose there is a despin mechanism which is covered during atmospheric exit by a fairing consisting of a portion of a torus along with small pyramidal fairings. The present investigation was conducted to determine the effect of two versions of the fairing shape for the despin mechanism on the longitudinal stability and to determine the fin size required to provide a statically stable exit configuration. The investigation was made on a 0.20-scale model in the Langley Unitary Plan wind tunnel at Mach numbers from 2.30 to 4.65. Results of this investigation are presented without analysis.

SYMBOLS

All coefficients are referred to the body system of axes shown in figure 1. The reference center for the center of pressure and the pitching-moment coefficients is located 6.565 base diameters ahead of the base of the model. The

coefficients are based on the cross-sectional area and diameter of the model third stage.

A	cross-sectional area of model third stage, 0.05918 sq ft
C_A	axial-force coefficient, $\frac{\text{Axial force}}{qA}$
C_m	pitching-moment coefficient, $\frac{\text{Pitching moment}}{qAd}$
C_{m_α}	stability parameter at $\alpha = 0^\circ$, $\frac{\partial C_m}{\partial \alpha}$
C_N	normal-force coefficient, $\frac{\text{Normal force}}{qA}$
C_{N_α}	normal-force-effectiveness parameter at $\alpha = 0^\circ$, $\frac{\partial C_N}{\partial \alpha}$
d	reference length (diameter of model third stage), 3.294 in.
M	Mach number
q	free-stream dynamic pressure
$\frac{x_{cp}}{d}$	center-of-pressure location in body diameters, positive upstream
α	angle of attack, deg

MODELS AND APPARATUS

Details of the body and the small and large fairing rings are presented in figure 2(a), and details of the small and large fins are shown in figure 2(b). The model was machined from solid aluminum and was supported in the tunnel by a sting and an internal strain-gage balance.

TESTS

Tests were made at angles of attack from about -7° to 7° at an angle of sideslip of 0° and at Mach numbers of 2.30, 2.96, 3.96, and 4.65. The configurations tested included the body with and without either of two fin sizes and either of two fairing rings. A transition strip consisting of No. 80 sand grains was located 1 inch aft of the nose of the model. The test Reynolds number was 2×10^6 per foot for all Mach numbers of the investigation.

CORRECTIONS AND ACCURACY

The angles of attack have been corrected for the flow angularity which exists in the vertical plane of the test section and the deflection of the balance-sting combination under load. No base-pressure correction to the forces has been made. The accuracies of the data are estimated to be:

C_N	±0.02
C_A	±0.005
C_m	±0.05

PRESENTATION OF RESULTS

Typical schlieren photographs of the model and flow field are presented in figure 3. The basic test results of the investigation of the longitudinal stability characteristics of the third and fourth stages of the SOCS launch vehicle with a cone-cylinder nose are presented in figure 4. Some results are summarized in figure 5. An outline of the data figures is as follows:

Aerodynamic characteristics in pitch for:

	Figure
Body alone	4(a)
Body with small ring	4(b)
Body with large ring	4(c)
Body with small fins	4(d)
Body with large fins	4(e)
Body with small ring and large fins	4(f)
Body with large ring and small fins	4(g)
Body with large ring and large fins	4(h)
Variation of longitudinal parameters with Mach number	5

SUMMARY OF RESULTS

A detailed discussion of results obtained in the investigation of the longitudinal stability characteristics of the final two stages of the four-stage SOCS launch vehicle has been omitted. However, the following general observations concerning the results of the present investigation are made.

The presence of the fairing rings had little effect on the longitudinal parameters C_{m_α} and C_{N_α} (fig. 5(b)), although the addition of the rings did cause some increase in axial-force coefficient (fig. 4). The addition of the fins, of course, provides a substantial increment in C_{N_α} and C_{m_α} that increases as the fin size is increased. (See fig. 5(b).)

A comparison of the center-of-pressure locations obtained from the tunnel tests with the predicted flight center-of-gravity locations for the SOCS launch vehicle (fig. 5(a)) indicates positive stability for the small-fin configurations up to about $M = 3.8$, above which the configuration becomes essentially neutrally stable with the small ring on or unstable with the large ring on. The configuration with the large fins provides a satisfactory margin of stability throughout the Mach number range of the investigation both with and without the fairing rings.

The large change in axial-force coefficient with Mach number for all the configurations (fig. 4) is due in part to the lack of base-pressure correction.

Langley Research Center,
National Aeronautics and Space Administration,
Langley Station, Hampton, Va., November 5, 1963.

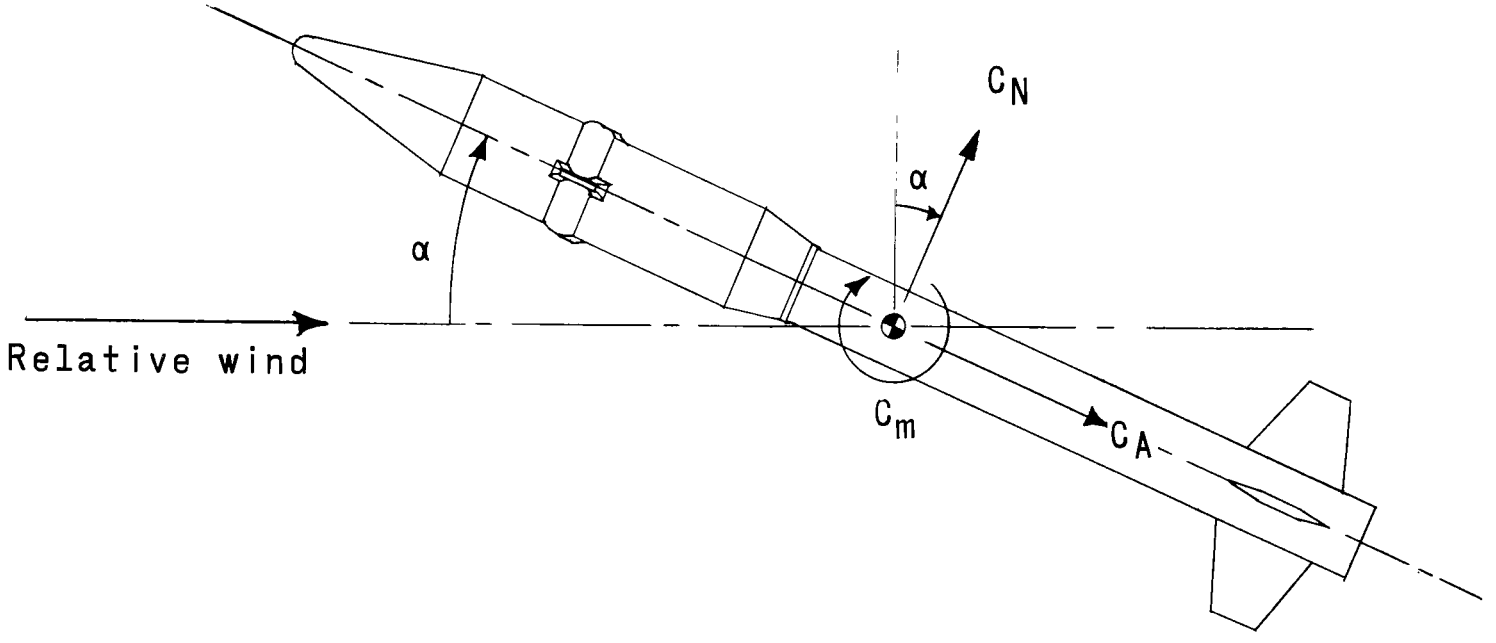

Figure 1.- System of axes. Positive directions are indicated by arrows.

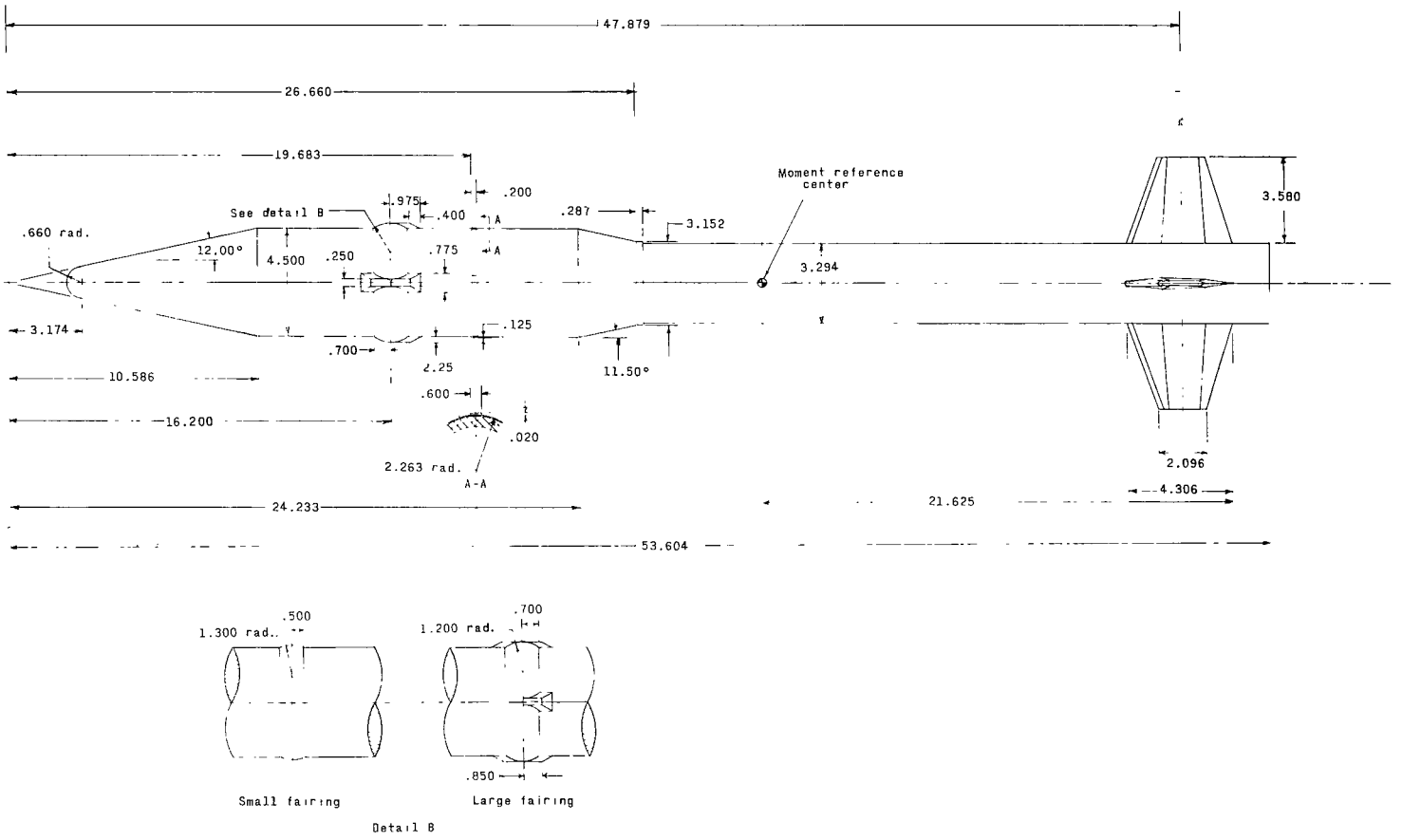

(a) Body and ring details.

Figure 2.- Details of models. (Dimensions are in inches unless otherwise noted.)

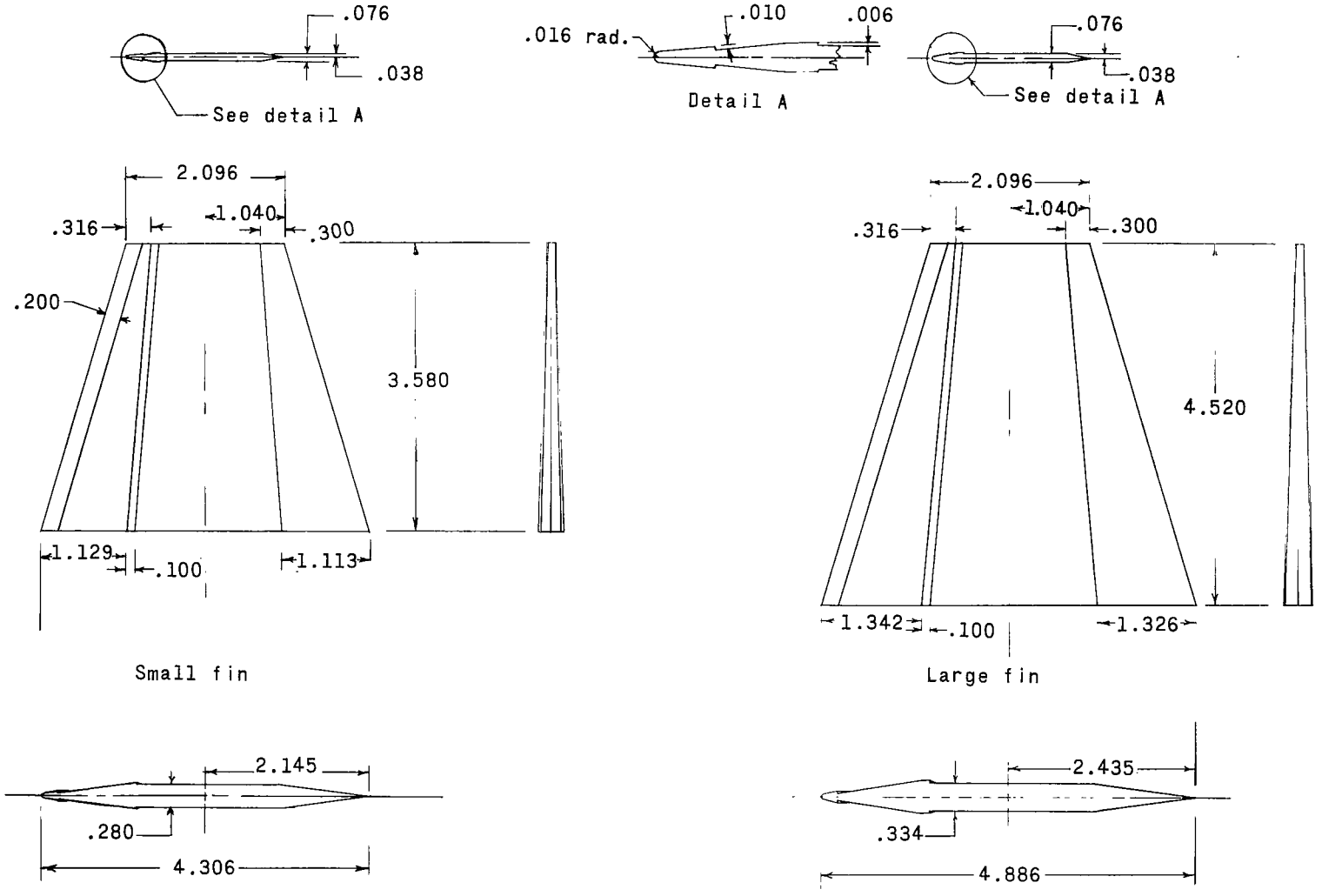

(b) Fin details.

Figure 2.- Concluded.

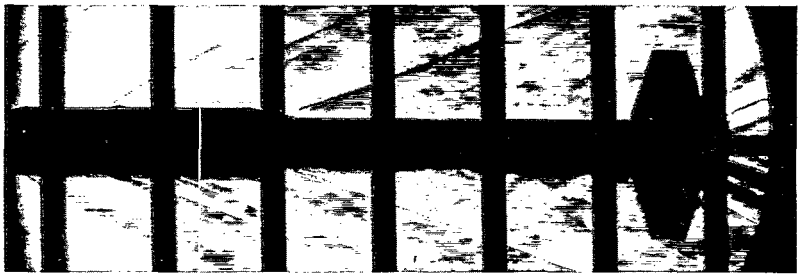

M = 2.30

M = 2.96

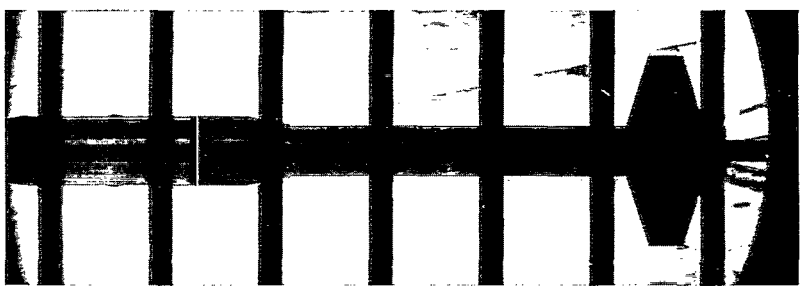

M = 3.96

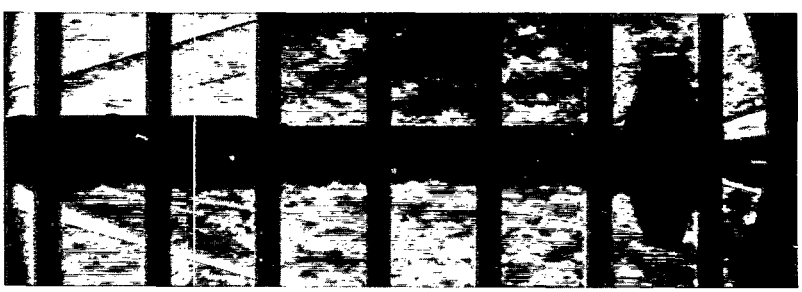

M = 4.65

(a) Small ring and large fins. L-63-9242

Figure 3.- Schlieren photographs with $\alpha \approx 0^{\circ}$.

M = 2.30

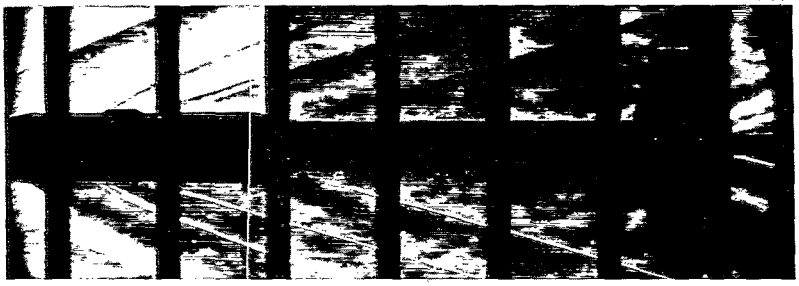

M = 2.96

M = 3.96

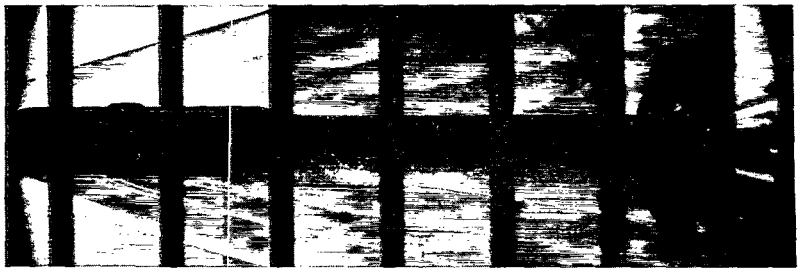

M = 4.65

(b) Large ring and large fins. L-63-9243

Figure 3.- Concluded.

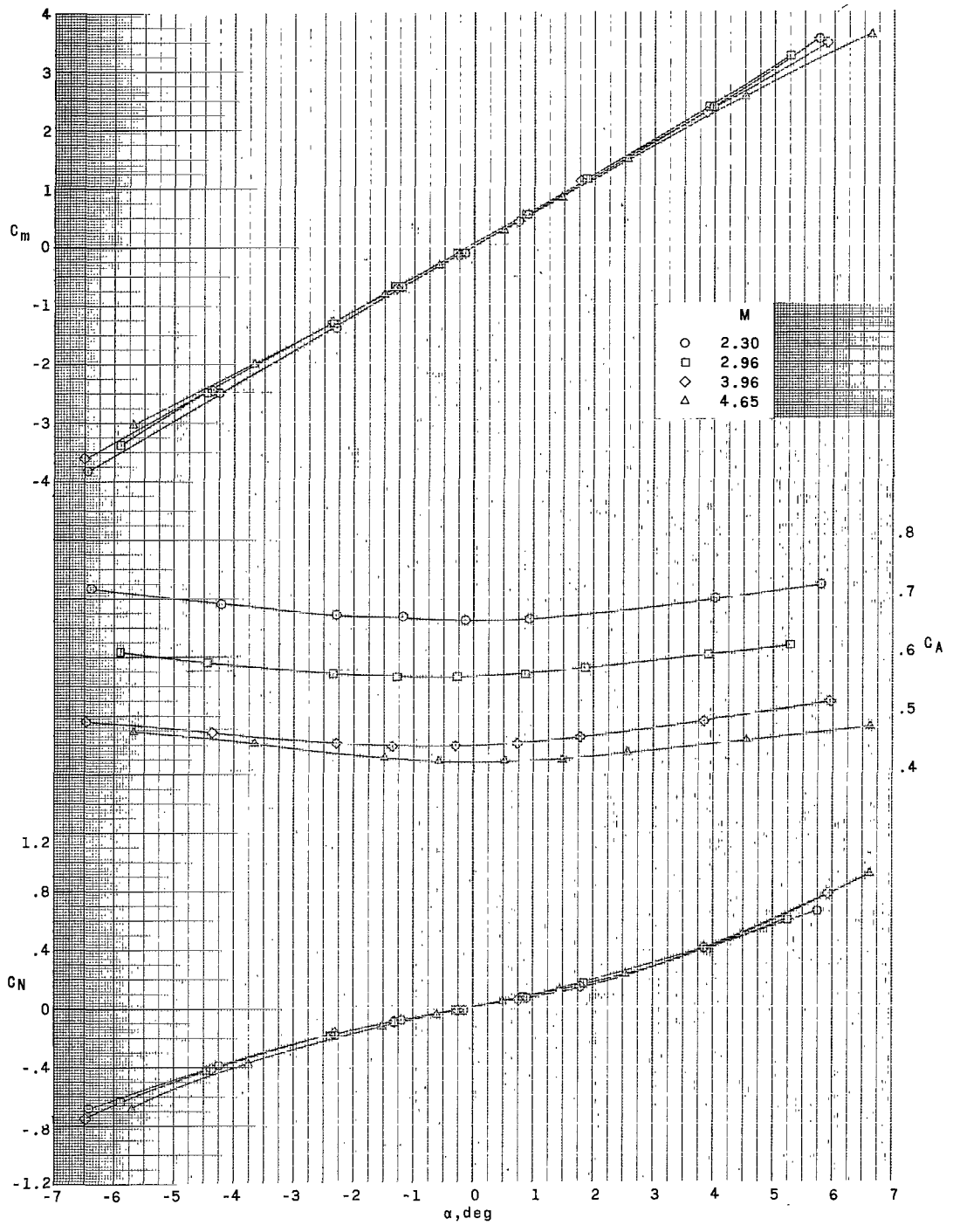

(a) Body alone.

Figure 4.- Aerodynamic characteristics in pitch for various configurations.

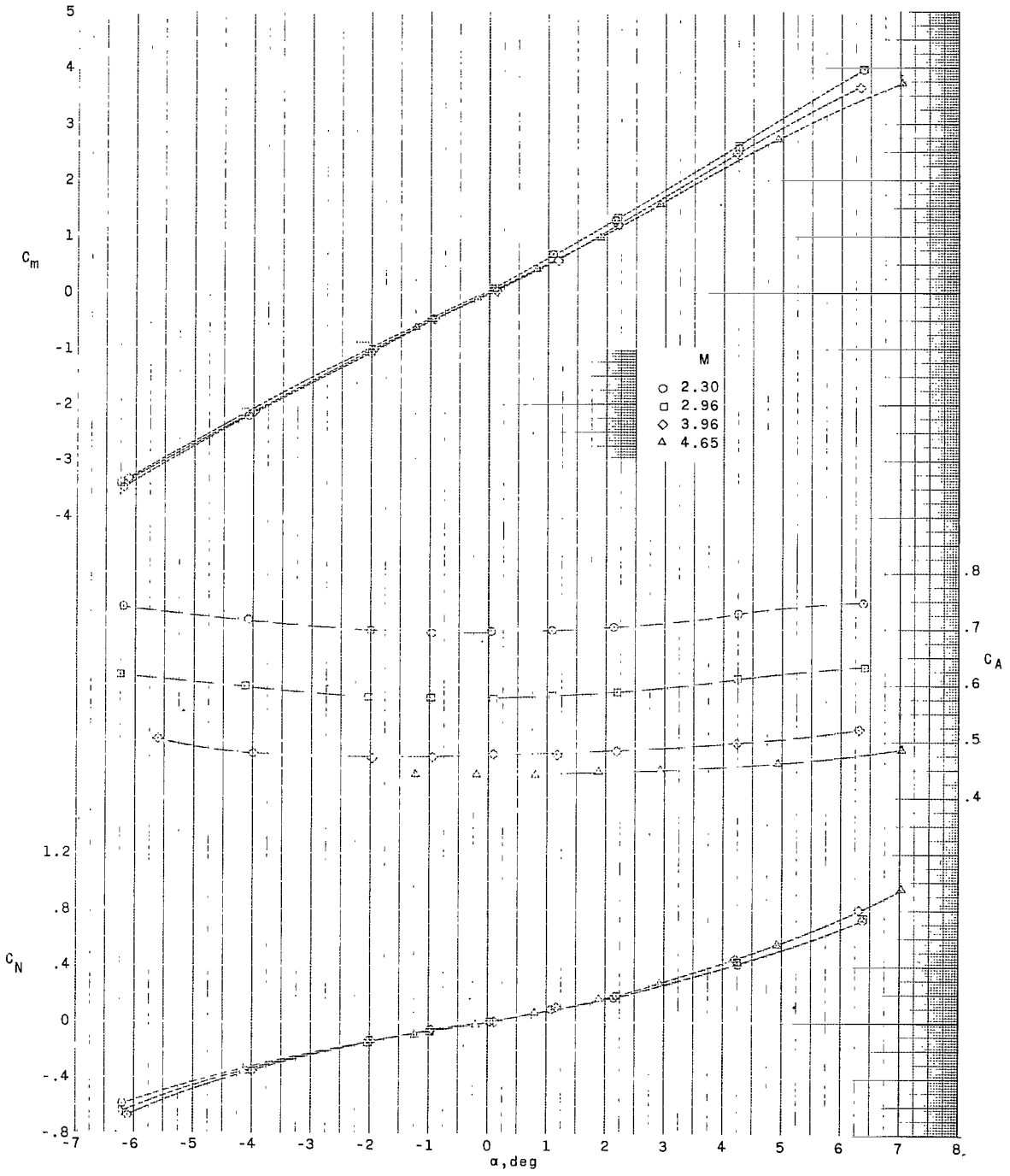

(b) Body with small ring.

Figure 4.- Continued.

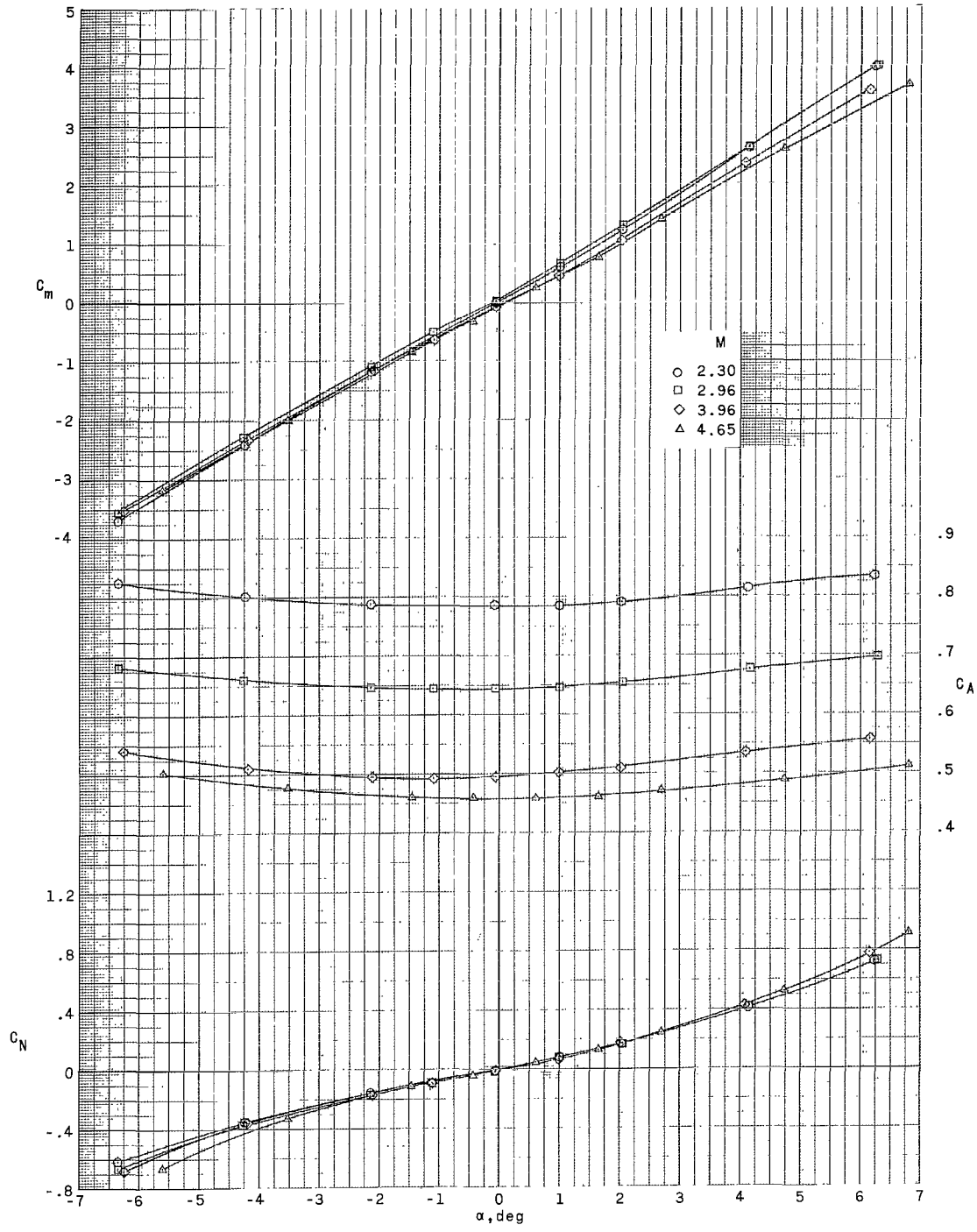

(c) Body with large ring.

Figure 4.- Continued.

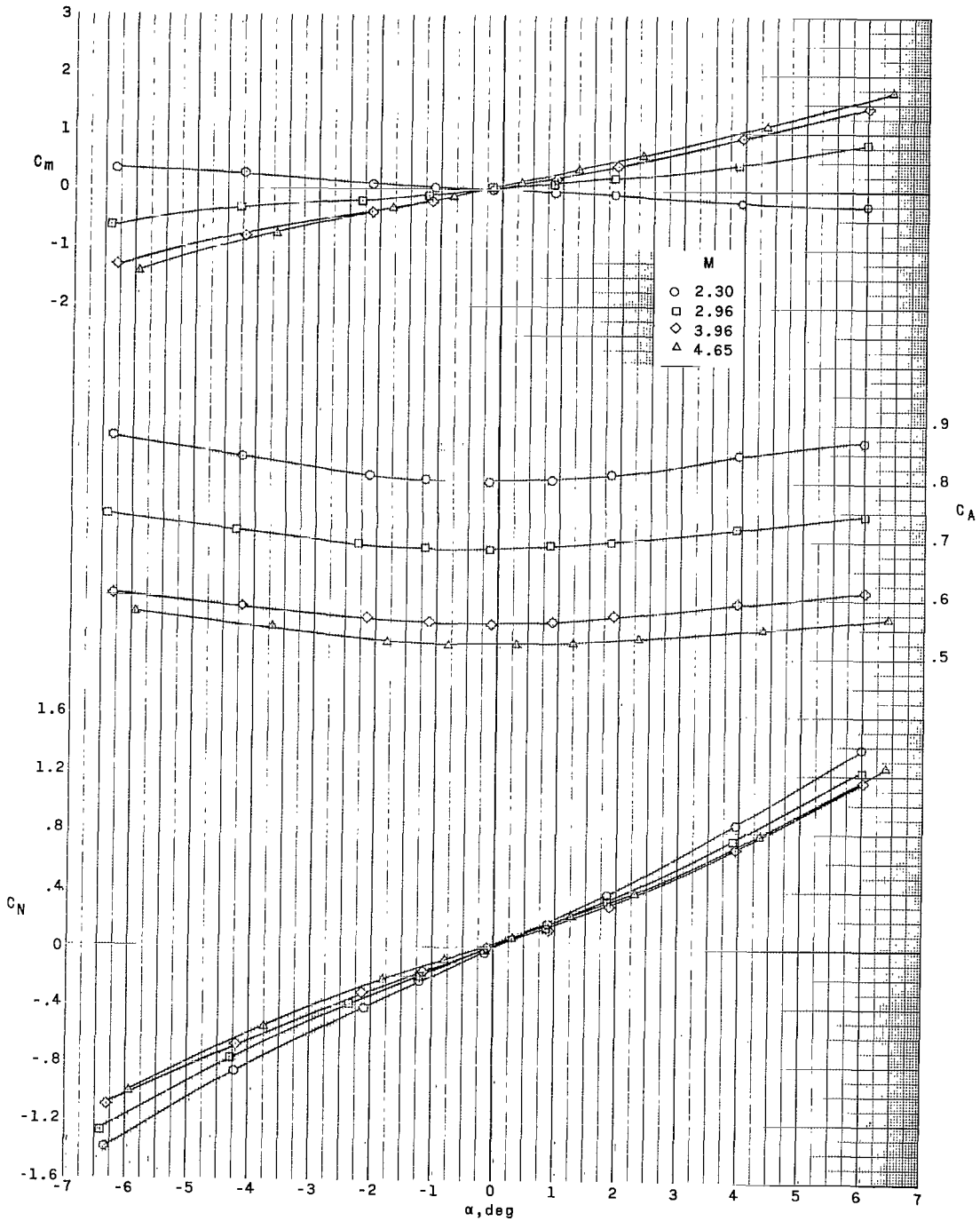

(d) Body with small fins.

Figure 4.- Continued.

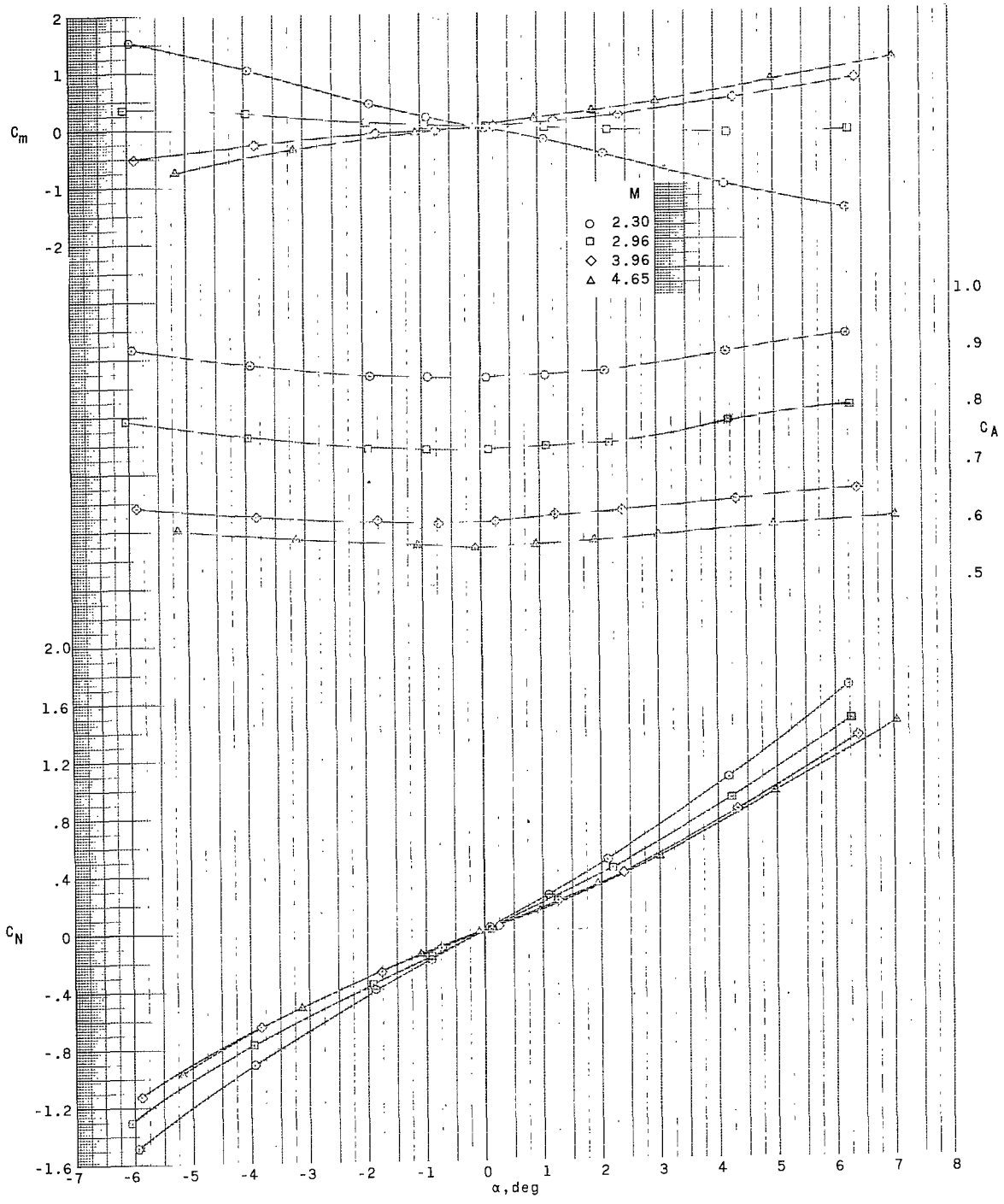

(e) Body with large fins.

Figure 4.- Continued.

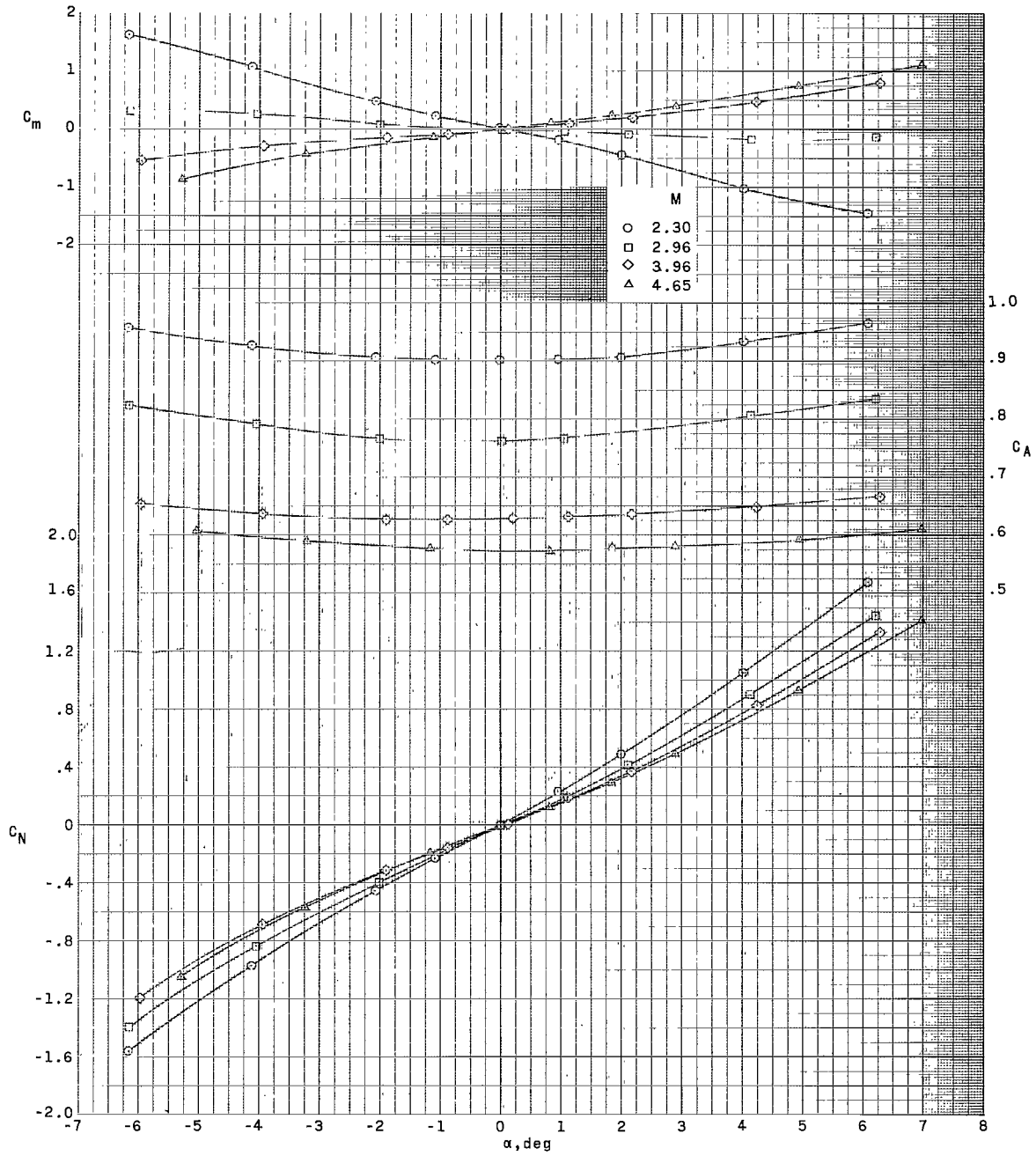

(f) Body with small ring and large fins.

Figure 4.- Continued.

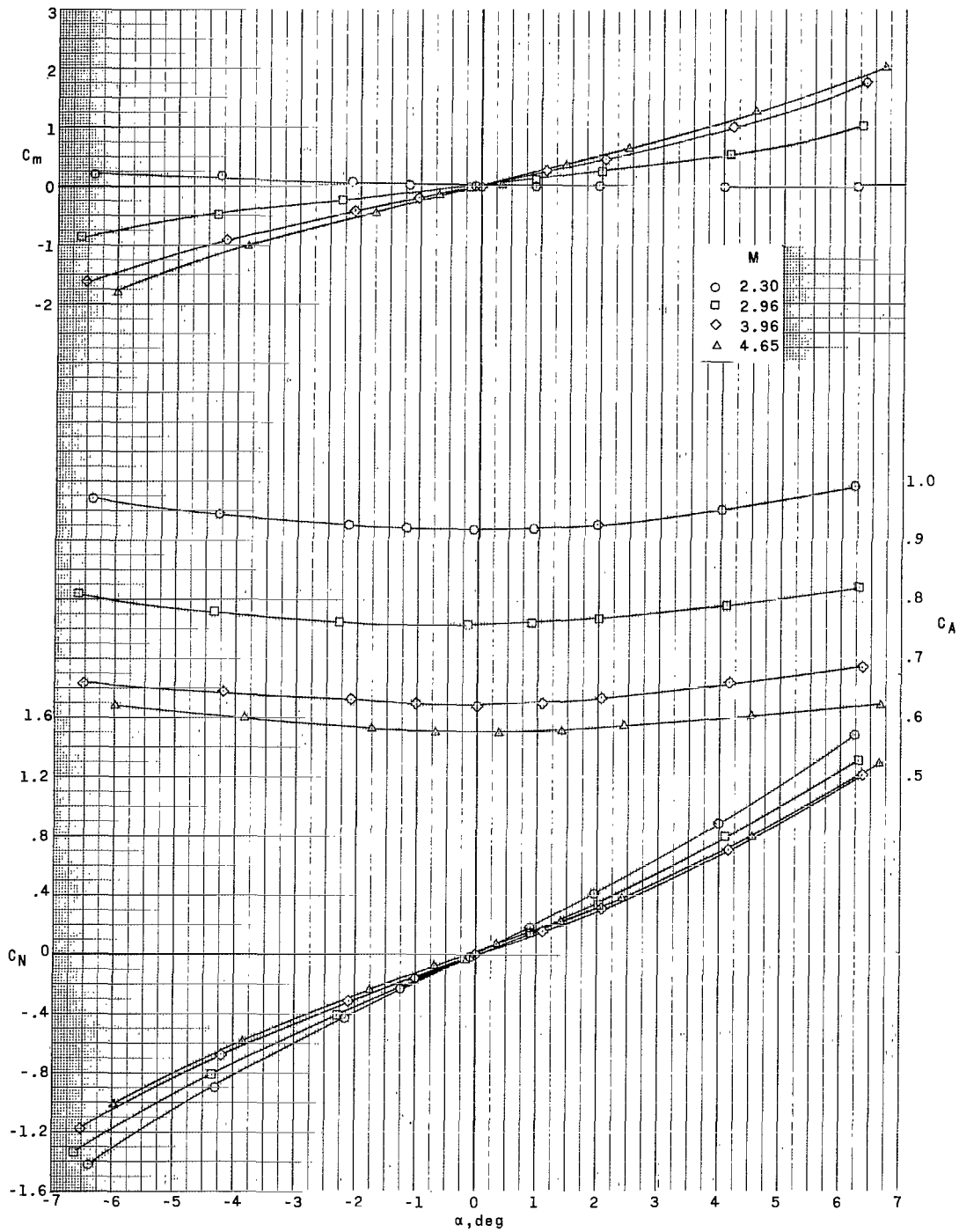

(g) Body with large ring and small fins.

Figure 4.- Continued.

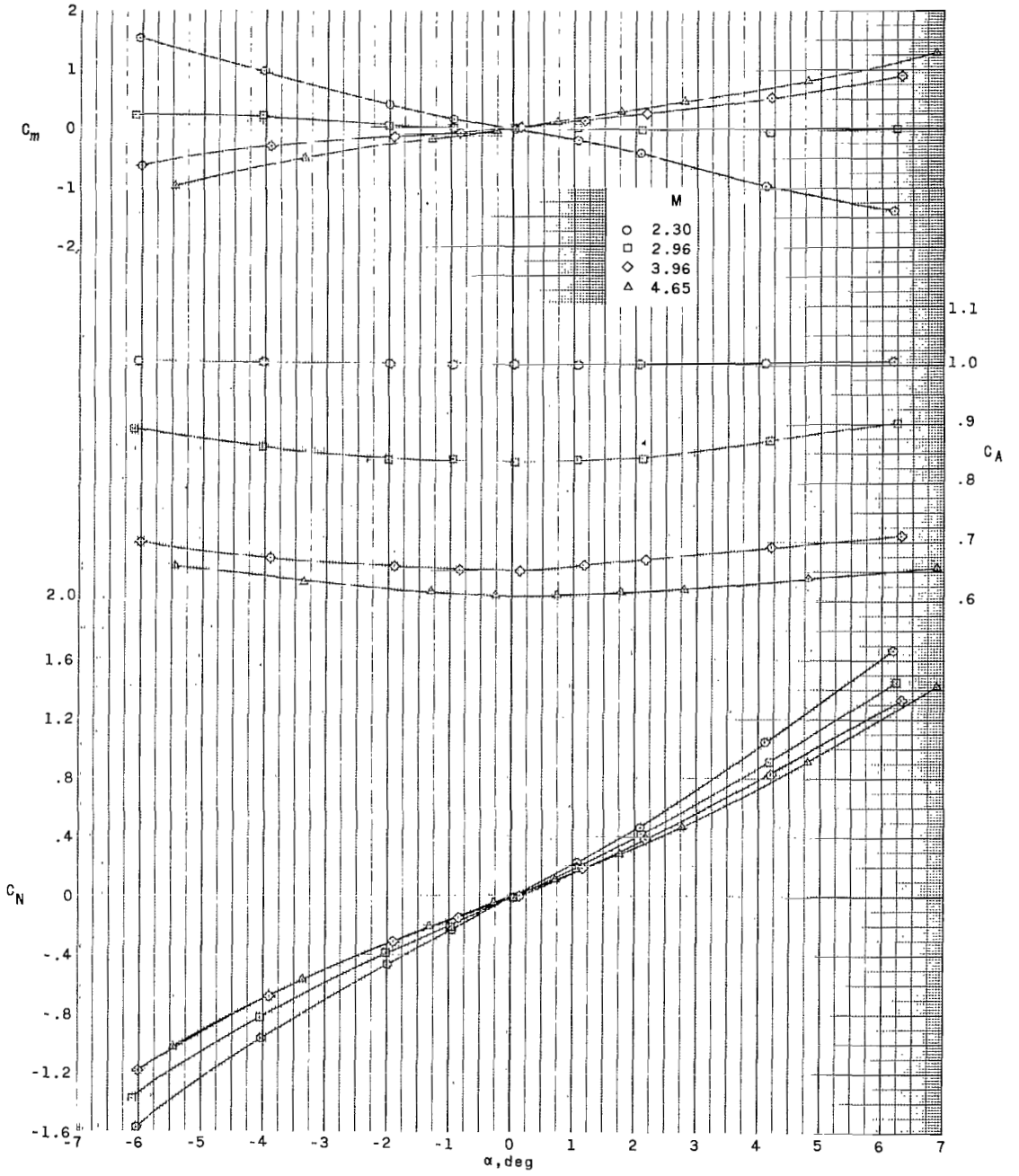

(h) Body with large ring and large fins.

Figure 4.- Concluded.

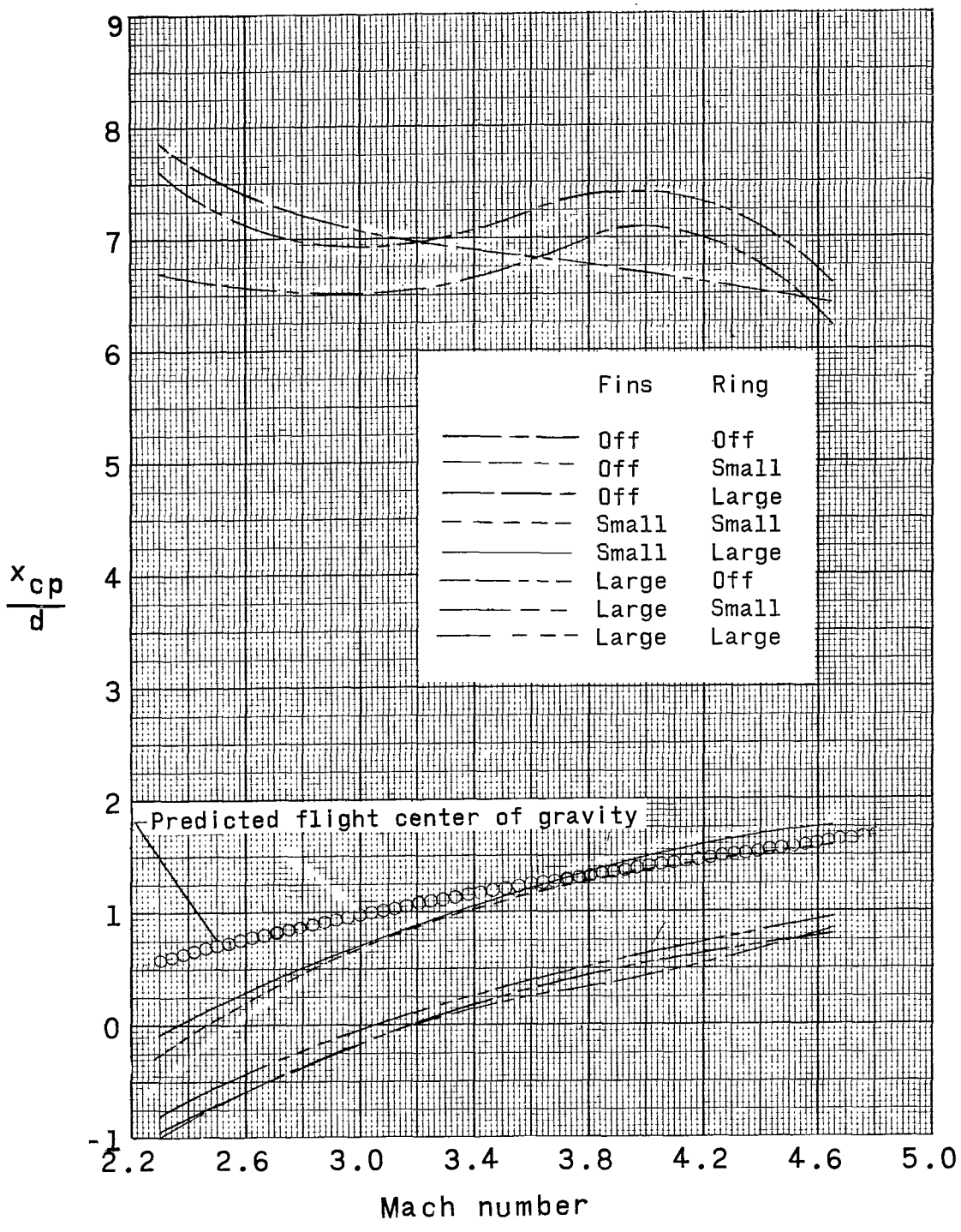

(a) Comparison of center of pressure with predicted flight center of gravity.

Figure 5.- Summary of aerodynamic characteristics in pitch for various configurations.

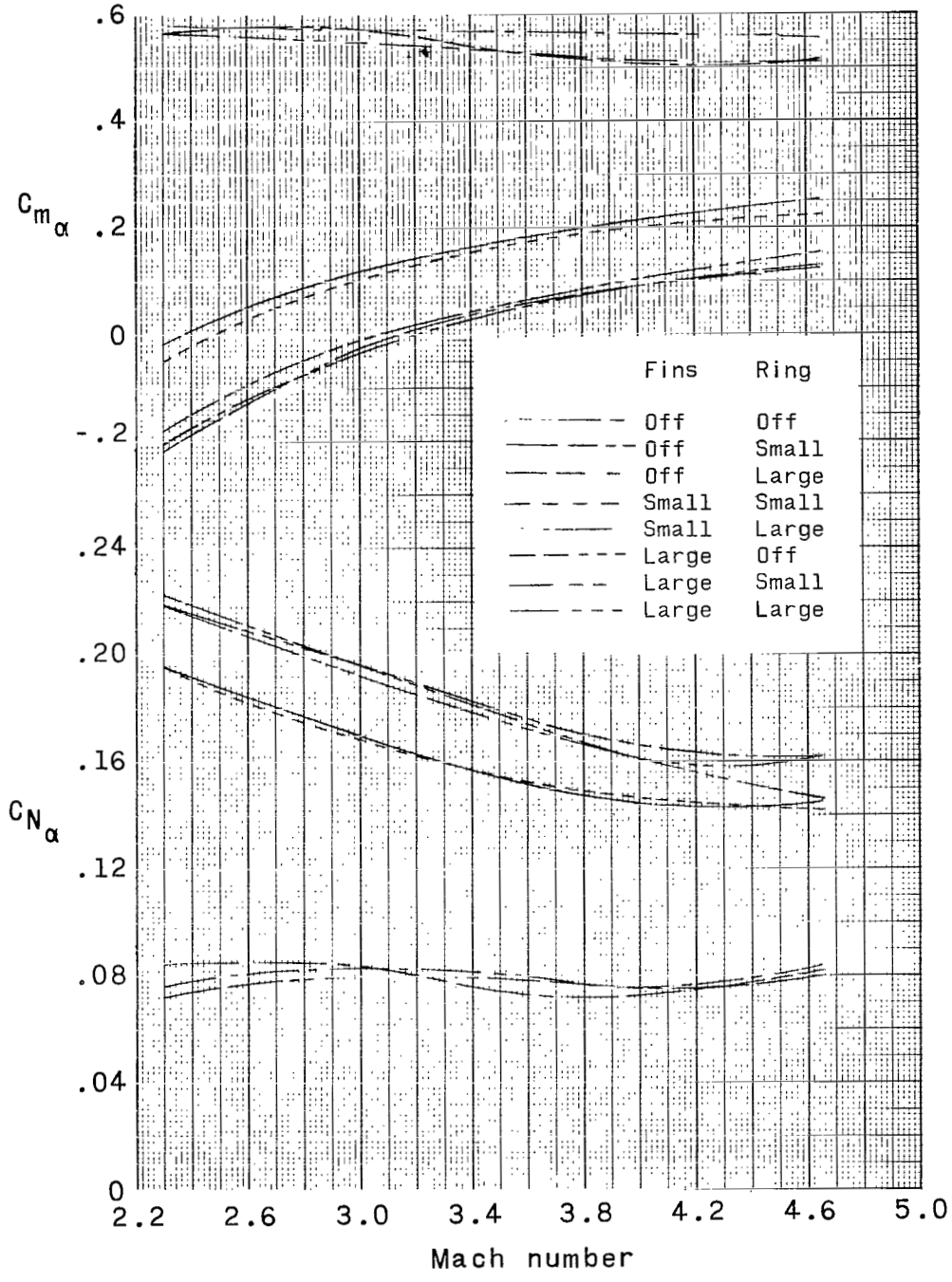

(b) Variation of stability parameter C_{m_α} and normal-force-effectiveness parameter C_{N_α} with Mach number.

Figure 5.- Concluded.

2/9/25